EGYPTIAN FIGURINE OF MAN WITH BABOON - ÆIN 784 - LEADED BRONZE - 3RD INTERMEDIATE PERIOD TO LATE PERIOD

Artefact name Egyptian figurine of man with baboon - ÆIN 784

Authors Ida. Langemark (The Royal Danish Academy, Copenhagen, Capital Region, Denmark)

Url /artefacts/1619/

The object



Fig. 1: Face, back and side views of the figurine,

Credit The Royal Danish Academy, I.Langemark.

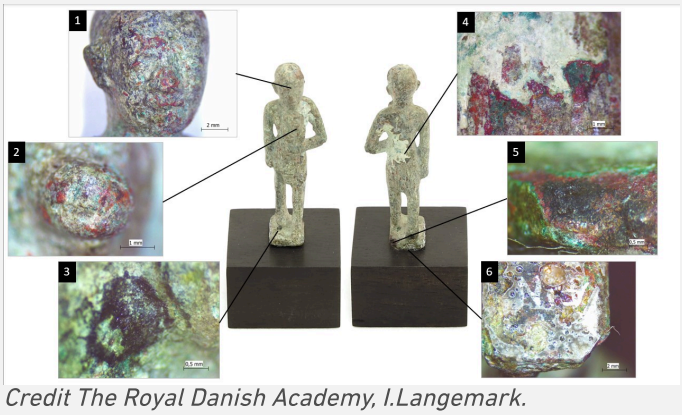


Fig. 2: Dark brown patina with light green powdery corrosion products on the surface (details),

Credit The Royal Danish Academy, I.Langemark.

Description and visual observation

Description of the artefact

The figurine depicts a man carrying a baboon figure, which was probably a sacrifice to the god Thoth. He is wearing a short kilt and a close-fitting hood, and was probably originally part of a composite statuette, where a god, crafted in a much larger scale, was the main motif of the work (Jørgensen, Ægypten V, 2009, p. 282). Height=5.8cm; Width=2.0cm; Thickness=1.8cm.

The surface is covered with a white substance with green impurities, located on top of corrosion layers of green, turquoise, red, and dark brown, especially prominent on the figure's

This work is licensed under CC BY-NC-ND 4.0

back (Fig. 2, picture 4). The proper left corner on the rear side of the figure's base has been damaged, and the stratigraphy can be easily distinguished (Fig. 2, picture 5).
There are residues of glue under the standing plate (Fig. 2, picture 6).

Type of artefact	Votive figure
Origin	Archaeological, ancient Egypt, exact provenance unknown
Recovering date	Recovered late 19th century
Chronology category	3rd Intermediate Period to Late Period
chronology tpq	1080 B.C.
chronology taq	300 B.C.
Chronology comment	None.
Burial conditions / environment	Unknown
Artefact location	Ny Carlsberg Glyptotek, Copenhagen
Owner	Ny Carlsberg Glyptotek, Copenhagen
Inv. number	ÆIN 784
Recorded conservation data	N/A

Complementary information

Mounted to wooden plinth.
Inventory number applied in white ink of unknown composition.

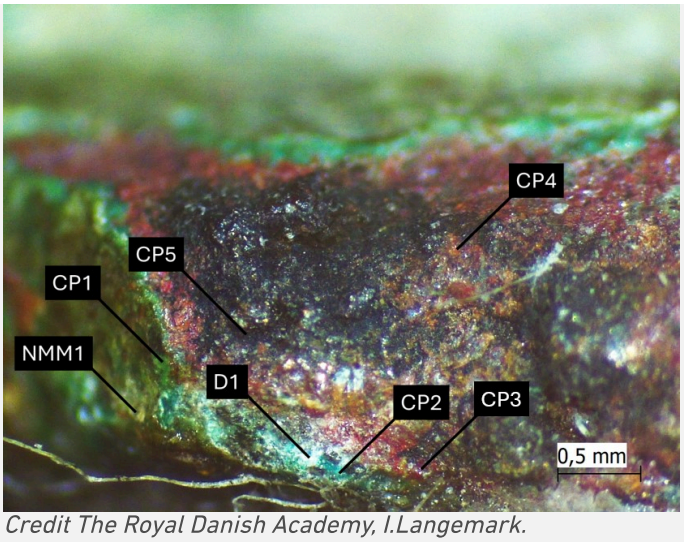
Study area(s)



Credit The Royal Danish Academy, I.Langemark.

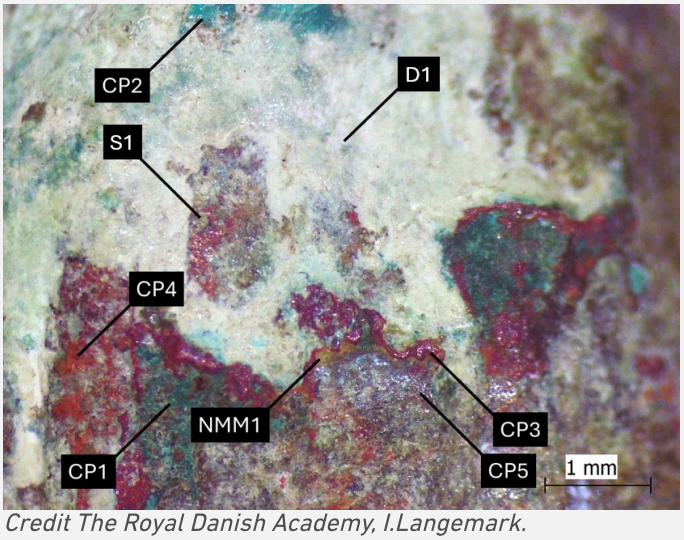
Fig. 3: Details of the strata of the corrosion structure as observed under binocular microscopy,

This work is licensed under CC BY-NC-ND 4.0



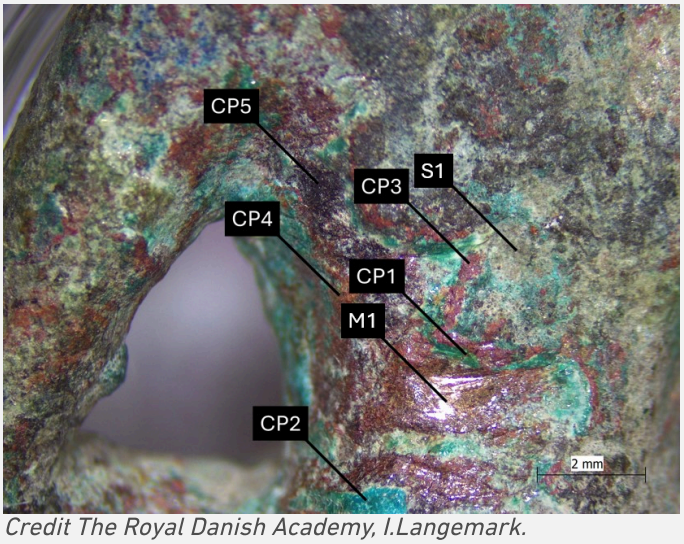
Credit The Royal Danish Academy, I.Langemark.

Fig. 4: Distribution of strata on the damaged part of the standing plate (Fig. 2, picture 5) observed under binocular microscopy,



Credit The Royal Danish Academy, I.Langemark.

Fig. 5: Distribution of strata on the light area on the back (Fig. 2, picture 4) observed under binocular microscopy,



Credit The Royal Danish Academy, I.Langemark.

Fig. 6: Distribution of strata on the back (detail) after superficial cleaning observed under binocular microscopy,

This work is licensed under CC BY-NC-ND 4.0



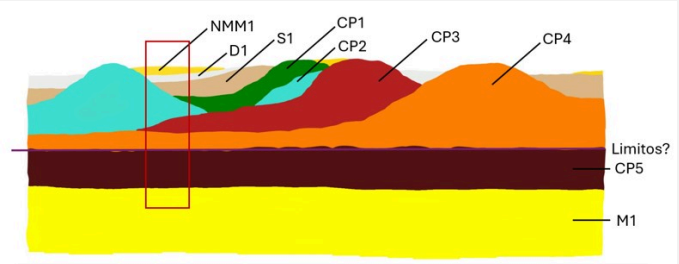
Credit The Royal Danish Academy, I.Langemark.

Fig. 7: Location of XRF measurements,

Binocular observation and representation of the corrosion structure

Stratigraphic representation:

The schematic representation below gives an overview of the corrosion structures encountered on the figurine from a first visual macroscopic observation.



Captions	Colour, aspect, hardness and cohesion
NMM1	Yellow waxy substance. Translucent, loosely adhered to underlying layer. Can be removed in malleable flakes.
D1	White, matte, powdery substance with green impurities. Very loosely adhered to underlaying layer.
S1	A thin, light brown layer. Loosely adhered to underlaying layer.
CP1	Green corrosion layer. Semi-translucent and reflective. Removes in brittle flakes when shaved with a scalpel blade.
CP2	Turquoise corrosion layer. Semi-translucent and reflective. Removes in brittle flakes when shaved with a scalpel blade.
CP3	Dark red corrosion layer, matte or with adamantine shine. Powdery under action of a scalpel blade.
CP4	Orange corrosion products located beneath CP3, directly on top of CP5. Powdery under action of a scalpel blade.
CP5	Dark brown and very hard corrosion layer that covers the entire figure. Matte or slightly reflective surface. Traces of engravings.
M1	Leaded bronze.

Credit The Royal Danish Academy, I.Langemark.

Fig. 8: Stratigraphic representation of the corrosion structure of the figurine by macroscopic and binocular observation, with indication of the corrosion structure used to build the MiCorr stratigraphy of Fig. 9 (red rectangular),

MiCorr stratigraphy(ies) – Bi

This work is licensed under CC BY-NC-ND 4.0

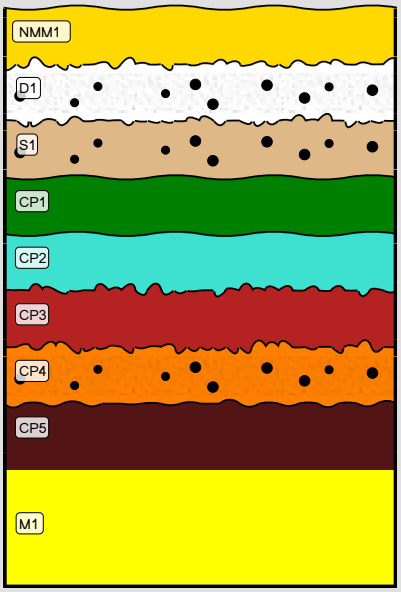
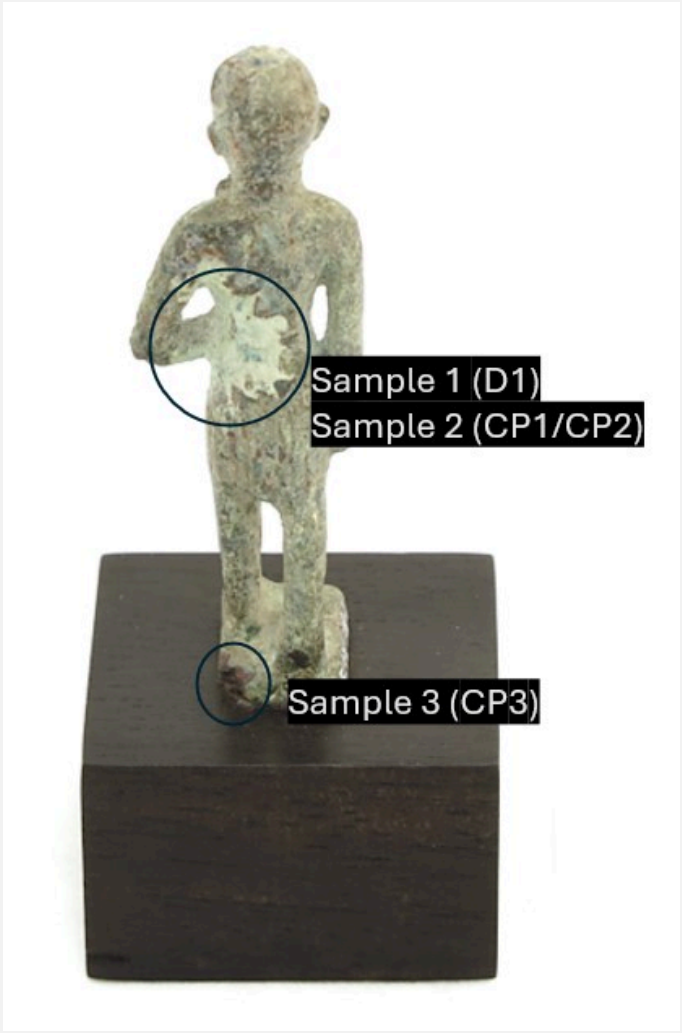


Fig. 9: Stratigraphic representation of the corrosion structure of the figurine observed macroscopically under binocular microscope using the MiCorr application. Credit The Royal Danish Academy, I.Langemark.

Sample(s)



Credit The Royal Danish Academy, I.Langemark.

Fig. 10: The back of the figurine showing the three sampling areas,

This work is licensed under CC BY-NC-ND 4.0

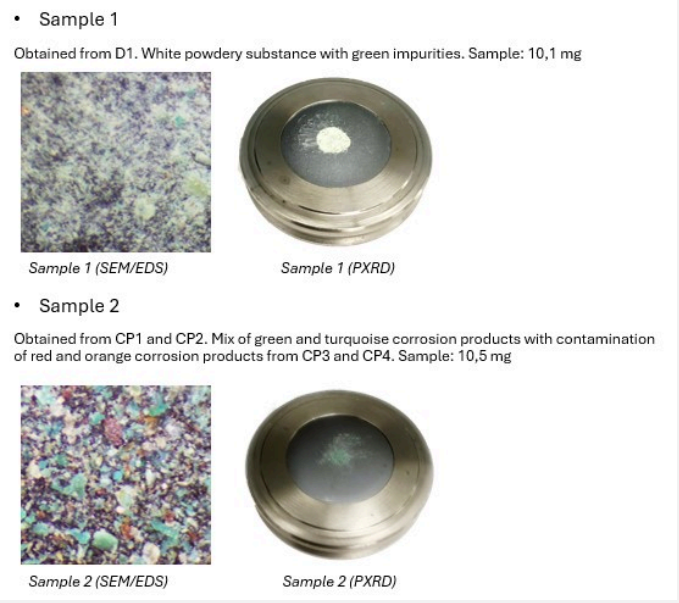


Fig. 11: Samples 1 and 2 observed under binocular microscope before SEM-EDS (left) and macroscopically before PXRD (right),

Credit The Royal Danish Academy, I.Langemark.

Description of sample	Three samples were taken to be analysed with SEM-EDS and PXRD from areas shown in Fig. 10. Four samples (1>mg) were observed under polarized microscopy, including material from D1 and C1-C4 (Figures 12-15).
Alloy	Leaded Bronze
Technology	Cast
Lab number of sample	
Sample location	The Royal Danish Academy (Langemark Ida), Copenhagen
Responsible institution	The Royal Danish Academy (Langemark Ida), Copenhagen
Date and aim of sampling	January 26th 2024, chemical and molecular analyses of corrosion products.

Complementary information

None.

Analyses and results

Analyses performed:

Non-invasive approach

- Portable micro-X-ray fluorescence (μ-XRF) on different measuring locations across the metal surface (Fig. 7). Measurements were made with a portable Bruker Tracer 5G XRF, with an analysis time of 30 sec and a spot size of 8 mm, mode general metal.

Invasive approach

- Polarized microscopy on 4 samples (D1, CP1, CP2, and CP3).
A small amount (1>mg) of material was removed from the surface with scalpel under binocular microscope. The material was placed in a drop of Euparal, covered with an object glass, and left to dry for some days. The samples were observed with a Leica 750P-microscope, and micrographs obtained with the software LAS X.

- Powder X-Ray diffraction (PXRD) of 3 samples. Due to the amount of material required for PXRD-analysis, sampling was done on all areas with a sufficient amount of material, and subsequently grinded into fine powder. PXRD-

This work is licensed under CC BY-NC-ND 4.0

analyses were performed with a PANalytical X'Pert Pro diffractometer at the Faculty of Pharmacy, Physics and Chemistry, University of Southern Denmark. Measurements were obtained with the software Data collector, and subsequent data processing was done with the applications HighscorePlus and Match!3 respectively.

- Scanning electron microscopy /Energy Dispersive X-ray Spectrometry (SEM-EDS) was performed on 2 samples. The samples were prepared by removing material from the surface with scalpel under binocular microscope. The sample material was attached to steel pins with double sided carbon tape. Analyses were performed with a Hitachi S - 3400N SEM-EDS, 15,0 kV and 300 sec at the Royal Danish Academy, Institute of Conservation.

Non invasive analysis

The µ-XRF-measurements have been performed on unpolished surface areas. They should be seen as indicative. Still the metal is a leaded bronze.

Measurement no.	Cu	Pb	Sn	Sb	Ag	Zn	Ni
1347	48.8	45.5	4.9	0.6	<	<	<
1348	38.9	54.2	6.0	0.8	<	<	<
1349	25.6	67.9	5.5	0.8	<	<	<
1350	34.9	56.8	7.3	0.9	<	<	<
1351	50.3	44.9	4.1	0.6	<	<	<

Table 1: Chemical composition (Elements mass (%)) of the figurine in the areas located on Fig. 7.

The µ-XRF-analysis shows a content of approx. 54 % (in weight) lead as an average of measurement 1347-1351. The lead content on the surface of the metal is rather high. The average tin-content is 6,5 %. µ-XRF-measurements show and average of 0,7 % antimony.

Metal

None.

Microstructure none

First metal element Cu

Other metal elements Sn, Sb, Pb

Complementary information

None.

Corrosion layers

The entire metal surface is covered with a dark brown patina, itself covered with various types of corrosion products, mostly Robbiola type I.

Five corrosion products and two non-metallic substances have been identified and can be visualised on Fig. 3 and Fig. 8.

This work is licensed under CC BY-NC-ND 4.0

As a reminder:

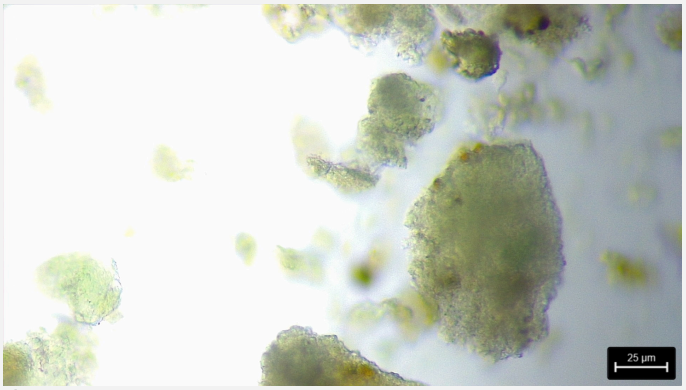
- NMM1: a yellow waxy substances, presumably remains of coating,
- D1: a white powdery substance with green impurities (Fig. 12),
- S1: a thin light brown layer,
- CP1: a dense green layer (Fig. 13),
- CP2: a dense turquoise layer found at a few localized spots (Fig. 14),
- CP3: a hard red layer (Fig. 15),
- CP4: orange corrosion products located beneath CP4, directly on top of CP5,
- CP5: a dark brown and very hard corrosion layer, that contains corresponding markers to the limit of the original surface.

Sample 1, consisting of material obtained from D1, shows under PXRD-analysis the presence of chlorartinite $Mg_2(CO_3)Cl(OH)\cdot 3H_2O$ (Fig. 16), a chloride analog of the magnesium mineral artinite. The white mineral is colourless in transmitted light (Frost 2009), but can contain impurities from other compounds such as copper ions, giving it a greenish appearance.

Sample 2, consisting of material obtained from CP1 and CP2 with contamination from CP3 and CP4, shows under PXRD-analysis the presence of aragonite $CaCO_3$ (Fig. 17), a colorless to white or grey mineral, often stained with various hues by impurities, such as blue, green, or red, but colourless in transmitted light.

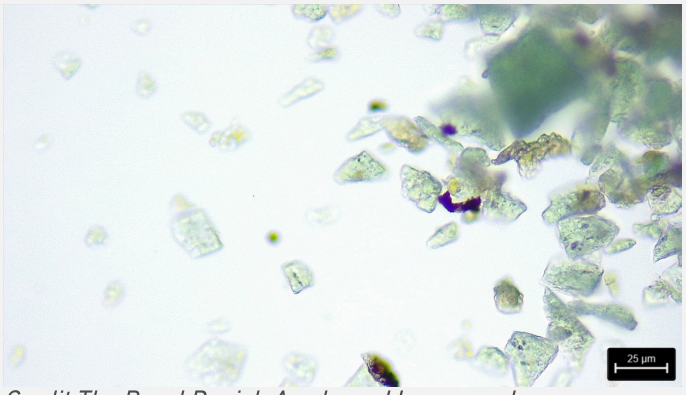
Sample 3, consisting of material obtained from CP3, shows under PXRD-analysis the presence of cuprite Cu_2O (Fig. 18), which is consistent with the characteristic red colour under polarized light (Fig. 15). The sample also contains clay minerals montmorillonite and sepiolite.

Sample 1 (D1) shows under EDS-analysis a significant amount of calcium with 24,14 % (weight percent) norm. C and some lead 7,78 % norm. C (Fig. 19). This could indicate that the white substance is a precipitation of a calcium compound contaminated with copper ions.
Sample 2 (CP1 and CP2) shows under EDS-analysis somewhat similar values, but a lower content of calcium of 17,72 % (weight percent) norm. C and a higher content of chlorine of 2,57 % norm. C (Fig. 20). This could indicate the presence of copper chloride compounds such as nantokite or copper trihydroxychlorides closer to the metal surface.



Credit The Royal Danish Academy, I.Langemark.

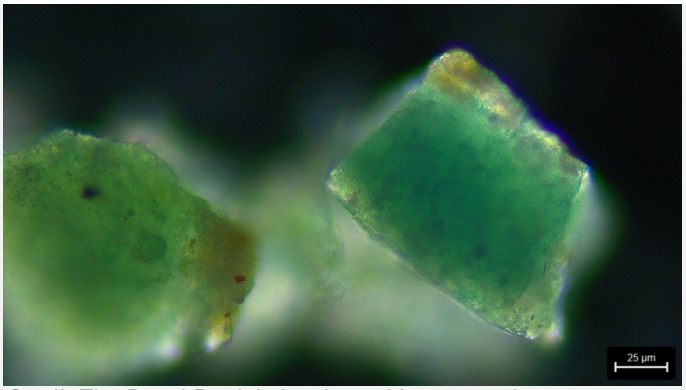
Fig. 12: Microscopic examination (bright field) of sample obtained from D1,



Credit The Royal Danish Academy, I.Langemark.

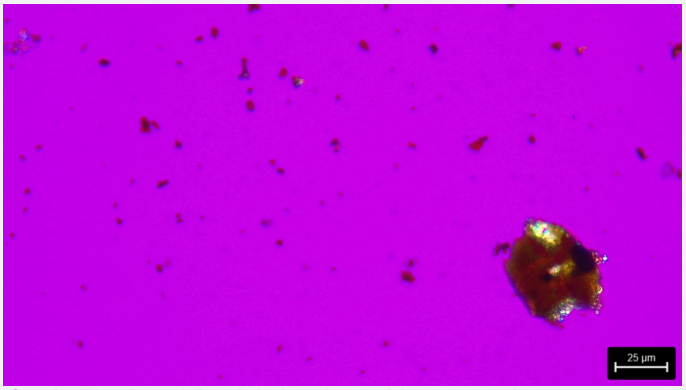
Fig. 13: Microscopic examination (bright field) of sample obtained from CP1,

This work is licensed under CC BY-NC-ND 4.0



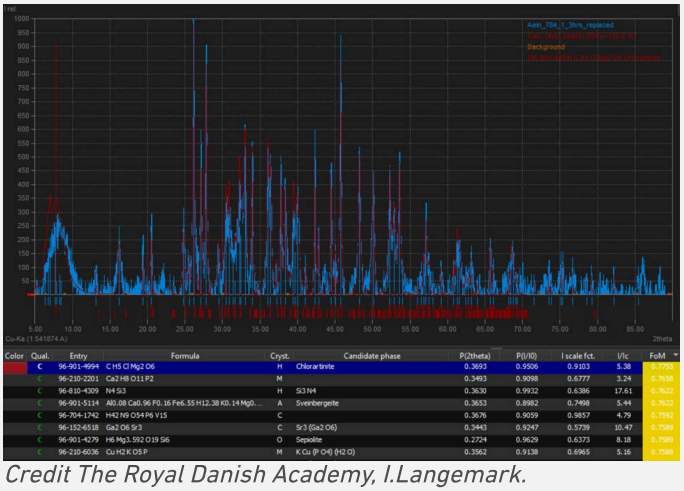
Credit The Royal Danish Academy, I.Langemark.

Fig. 14: Microscopic examination (crossed polars) of sample obtained from CP2,



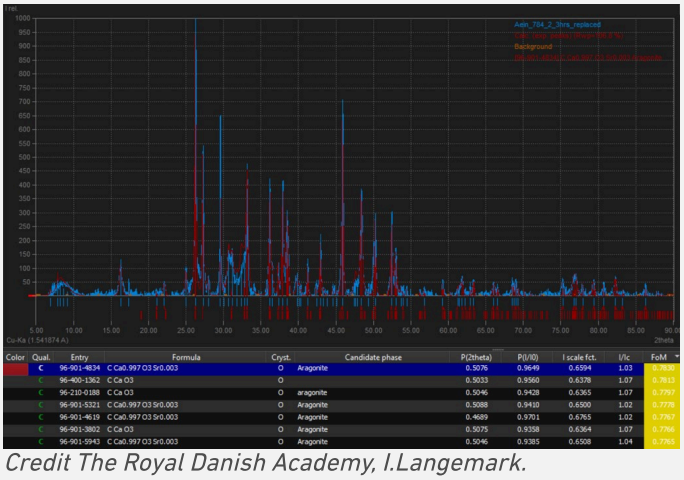
Credit The Royal Danish Academy, I.Langemark.

Fig. 15: Microscopic examination under polarized light of sample obtained from CP3,



Credit The Royal Danish Academy, I.Langemark.

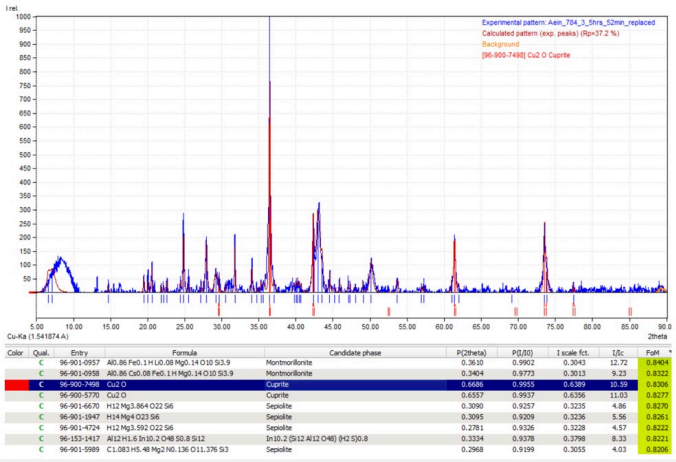
Fig. 16: XRD spectrum obtained from PXRD-analysis of Sample 1 obtained from D1, showing the presence of chlorartinite,



Credit The Royal Danish Academy, I.Langemark.

Fig. 17: XRD spectrum obtained from PXRD-analysis of Sample 2 obtained from CP1 and CP2, showing the presence of aragonite,

This work is licensed under CC BY-NC-ND 4.0



Color	Qual.	Entry	Formula	Candidate phase	P(2theta)	P(I,I0)	I scale fct.	I/Ic	FoM
	C	96-901-0957	Al0.86 Fe0.1 H L0.08 Mg0.14 O10 Si3.9	Montmorillonite	0.3610	0.9902	0.3043	12.72	0.8404
	C	96-901-0958	Al0.86 Ca0.08 Fe0.1 H Mg0.14 O10 Si3.9	Montmorillonite	0.3404	0.9773	0.3013	9.23	0.8322
	C	96-900-7498	Cu2 O	Cuprite	0.6686	0.9955	0.6389	10.59	0.8306
	C	96-900-5770	Cu2 O	Cuprite	0.6557	0.9937	0.6356	11.03	0.8277
	C	96-901-6670	H12 Mg3.864 O22 Si6	Sepiolite	0.3090	0.9257	0.3235	4.86	0.8270
	C	96-901-1947	H14 Mg4 O23 Si6	Sepiolite	0.3095	0.9209	0.3236	5.56	0.8261
	C	96-901-4724	H12 Mg3.592 O22 Si6	Sepiolite	0.2781	0.9326	0.3228	4.57	0.8222
	C	96-153-1417	Al12 H1.6 In10.2 O48 S0.8 Si12	In10.2 (Si12 Al12 O48) (H2 S)0.8	0.3334	0.9378	0.3798	8.33	0.8221
	C	96-901-5989	C1.083 H5.48 Mg2 N0.136 O11.376 Si3	Sepiolite	0.2968	0.9199	0.3055	4.03	0.8206

Fig. 18: XRD spectrum obtained from PXRD-analysis of Sample 3 obtained from CP3, showing the presence of cuprite and clay minerals,

Credit The Royal Danish Academy, I.Langemark.

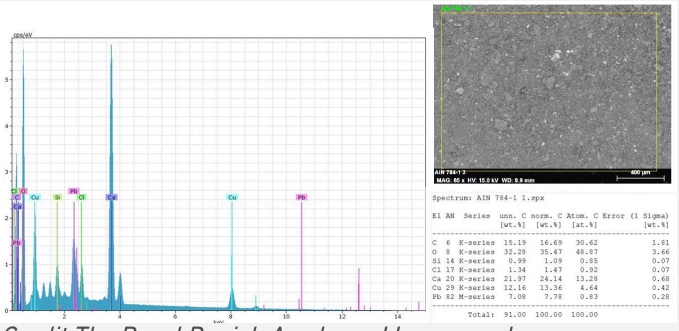


Fig. 19: Data from EDS-analysis of Sample 1,

Credit The Royal Danish Academy, I.Langemark.

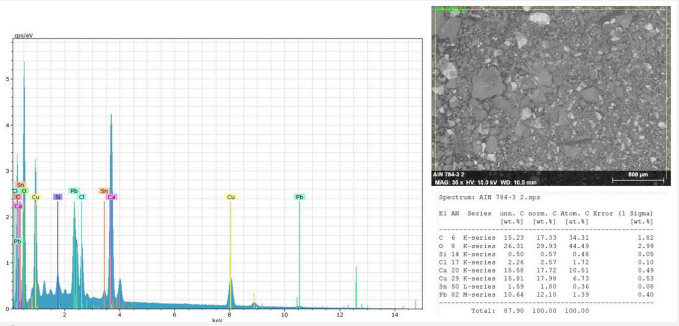


Fig. 20: Data from EDS-analysis of Sample 2,

Credit The Royal Danish Academy, I.Langemark.

Corrosion form Multiform

Corrosion type Mostly type I with locally type II (Robbiola)

Complementary information

None.

MiCorr stratigraphy(ies) – CS

Synthesis of the binocular / cross-section examination of the corrosion structure

None.

This work is licensed under CC BY-NC-ND 4.0

Conclusion

The figurine is a leaded bronze.

The corrosion products, which cover the entire object, are multi-layered. Most of the corrosion layers correspond to type I of Robbiola.

Three samples were analyzed with PXRD: chlorartinite was detected in a sample obtained from D1. Aragonite was detected in a sample obtained from CP1/CP2, with possible contamination from CP3 and CP4. PXRD-analysis verified CP3 as cuprite mixed with typical clay minerals.

EDS-analysis of material obtained from D1 and CP1 respectively both showed a high content of calcium, some lead, and chlorine. By comparing the data from EDS- and PXRD-analysis, chlorine is presumed to be present in the form of $Mg_2(CO_3)Cl(OH)\cdot 2.5H_2O$, the chloride analog of artinite (Frost et al. 2009), and not as nantokite or the tri-hydroxychloride often associated with active corrosion (Scott 2002).

However, the presence of magnesium compounds such as chlorartinite ($Mg_2(CO_3)Cl(OH)\cdot 2.5H_2O$) and aragonite ($CaCO_3$) may contract water from air humidity, and accelerate corrosion of the metal.

References

References on object and analytical methods

Reference object

1. Jørgensen, M. (2009) Katalog Ægypten V. Ny Carlsberg Glyptotek 2009, 97.1.
2. MiCorr_Figurine of Egyptian God Bes n°1 - AEIN 223

Reference analytical method

3. Frost, R. L. Bahfenne, S., Graham, J. (2009) Raman spectroscopic study of the magnesium-carbonate minerals-artinite and dypingite. Journal of Raman Spectrocopy, 40 (8). Pp. 855-860. doi: 10.1002/jrs.2152.
4. Scott, D. A. (2002) Copper and Bronze in Art - Corrosion, Colorants, Conservation, Getty Conservation Institute, Getty Publications, 2002.

This work is licensed under CC BY-NC-ND 4.0